Satellite SAR interferometric observations of displacements associated with urban subsidence in Suzhou, Eastern China*

WANG Chao[1]**, ZHANG Hong[1], LIU Zhi[1], CHENG Suozhong[2] and LÜ Guonian[2]

(1. LARSIS, Institute of Remote Sensing Applications, Chinese Academy of Sciences, Beijing 100101, China; 2. Department of Geography, Nanjing Normal University, Nanjing 210097, China)

Received January 9, 2002; revised February 1, 2002

Abstract SAR interferometry (InSAR) has a high potential for surface displacement mapping in the range from millimeter to meter. In this paper the potential of ERS-1/2 SAR interferometry for mapping subtle land subsidence has been investigated. A time series of ERS-1/2 SAR data from February 1993 to February 2000 is collected from measurements taken in Suzhou city, Jiangsu Province, China, eight ERS-1/2 SAR images are used to create seven interferograms, and three differential interferograms are produced using the three-pass method, which clearly show the spatial extent of land subsidence. The deformation maps are validated by leveling surveys, the correlation coefficient and standard deviation between them are 0.943 and 0.1706 respectively. Based on seven benchmarks, the subsidence rates are estimated, the overall trends are in close agreement with InSAR results. The results of study show that for the mapping of land subsidence in urban environments InSAR has a strong potential due to its cost-saving, high resolution and accuracy.

Keywords: SAR interferometry, land subsidence, Suzhou.

Land subsidence has occurred in nearly 50 cities of 16 provinces in China, which causes an economic loss of 0.1 billion RMB yuan annually. Suzhou is one of the most remarkable cases of urban land subsidence in China with regard to the extent of the subsiding area and to the velocity of the vertical movements. There is a strong demand for accurate and economical method to monitor land subsidence to effectively control the water overexploitation.

Traditional measurements of land subsidence are made by detailed surveying and tide gauges. Recently, GPS surveys and tiltmeters have been used. All of these techniques: (i) measure changes in locations of a limited set of benchmarks, (ii) require a large number of individual observations to map the subsidence distribution, (iii) require ground access, and (iv) are generally costly to acquire.

Geophysical applications of InSAR take advantage of the phase component of reflected radar signals to measure apparent changes on the ground surface. Interferograms, formed from patterns of interference between the phase components of two radar scans made from the same antenna position (viewing angle) but at different times, have demonstrated dramatic potential for high-density spatial mapping of ground surface deformations associated with tectonic and volcanic strains[1~9].

The aim of this study is to analyze the potential of InSAR as a tool for investigating subsiding areas and to validate the applicability of this method to proper areas. The analysis is made by comparing the SAR results with those of leveling surveys in order to validate a standard approach integrating the two survey methods. A time series of ERS-1 and ERS-2 SAR data form February 1993 to February 2000 and high precision leveling surveys of 1993 and 1995 will be analyzed.

1 Methodology

The interferometric phase is sensitive to both surface topography and coherent displacement along the look vector occurring between the acquisitions of the interferometric image pair. Inhomogeneous propagation delay and phase noise are the main error sources. The unwrapped interferometric phase ϕ_{unw} can be expressed as a sum of a topographic term ϕ_{topo}, a displacement term ϕ_{disp}, an atmospheric disturbance term ϕ_{atmo}, and a phase noise term ϕ_{noise}:

$$\phi_{unw} = \phi_{topo} + \phi_{disp} + \phi_{atmo} + \phi_{noise}. \quad (1)$$

The phase to height sensitivity is

* Supported by the Major State Basic Research Development Program of China (Grant No. G1998040703) and the Chinese Academy of Sciences (KZCX2-309). The ERS-1/2 SAR data was provided by ESA for the ERS project (ERS A03-374).

** E-mail: cwang@public.bta.net.cn

$$\delta\phi_{topo} = \frac{4\pi}{\lambda}\frac{B_\perp}{r\cos\theta}\delta h, \quad (2)$$

where λ is the wavelength; $B_\perp$ the baseline component perpendicular to the look vector; θ the incidence angle; and r the slant range. Knowing the baseline geometry and ϕ_{topo} and together with the orbit information allows us to calculate the 3-dimensional position of the scatter elements.

Displacement ϕ_{disp} is related to the coherent displacement of the scattering centers along the radar look vector r_{disp}:

$$\phi_{disp} = \frac{4\pi}{\lambda} r_{disp}. \quad (3)$$

Changes in the effective path length between the SAR and the surface elements as a result of changing permittivity of the atmosphere, caused by changes in the atmosphere conditions, lead to non-zero ϕ_{atmo}. Finally incoherent displacement of the scattering centers as well as noise introduced by SAR signal noise are the source of ϕ_{noise}. Multi-looking and filtering of the interferogram can reduce phase noise.

In the general case, $\phi_{topo} \neq 0$, surface displacement mapping requires the estimation of the topographic phase term. This is done on an independent digital elevation model by a two-pass approach or based on an independent interferogram with negligible (or known) surface displacement by a multi-pass approach[7].

2 Study area and ERS SAR data

2.1 Study area

The study area is situated in the central part of Suzhou, Eastern China, centered approximately at 31°20′N and 120°35′E. In the Suzhou urban areas, the ground altitude is generally less than 4 m and the lowest is between −3.0 m and 3.0 m. Since the 1980s the problem of land subsidence has become serious because of accelerating urban infrastructure construction associated with the rapid economic development. Groundwater is currently pumped at a rate two to three times more than the natural recharge, persistent overdraft of the aquifer system lowers water levels throughout Suzhou-Wuxi-Changzhou area, in some places in excess of 90 m. Until 1995 the maximum cumulative subsidence had been up to 1.45 m because of cumulative working of water overexploitation. The fastest descending rate is 40～50 mm/a, and the coverage reached 80.4 km^2. Recently the downtrend has been basically controlled through reducing ground water exploitation to a large extent and recharging of ground water.

2.2 ERS SAR data and processing

A time series of eight ERS-1/2 SAR scenes from February 1993 to February 2000 was analyzed (see Table 1). These data may compute seven interferograms with large acquisition time intervals and short perpendicular baselines. The main processing steps included SAR processing, interferometric processing, subtraction of topographic phase term using three-pass differential SAR interferometry, adaptive filtering, phase unwrapping, averaging of multiple results in order to reduce atmospheric disturbance.

Table 1. Temporal and perpendicular baseline parameters of seven interferometric pairs

No.	Reference orbit	Reference date	Interference orbit	Interference date	$B_\perp$(m)
1	E1-23309	1995/12/30	E2-3636	1995/12/31	−282
2	E1-23309	1995/12/30	E1-8436	1993/02/25	37
3	E1-23309	1995/12/30	E1-8937	1993/04/01	−11
4	E1-23309	1995/12/30	E1-24311	1996/03/09	−20
5	E2-3636	1995/12/31	E2-15660	1998/04/19	−48
6	E2-18165	1998/10/11	E2-15660	1998/04/19	−199
7	E2-18165	1998/10/11	E2-25179	2000/02/13	30

3 Results

Three differential interferograms for different time periods from February 1993 to February 2000 (Plate I) reveal spatial details about the temporal variation of subsidence. Each fringe in a subsidence feature represents a surface movement of 28 mm in the radar look direction. Features with at least one fringe are clearly visible in the image, provided that they occur in relatively coherent regions, indicating that the vertical measurement accuracy is at least a few centimeters, given favorable coherence conditions, or better ideal conditions.

These interferograms show that the subsidence is largely limited to the urban area, and almost distributed in the NE direction. The time series of deformation maps demonstrate that the subsidence area and velocity have descended because of the effective control of groundwater.

4 Ground validation

Initial results suggest that land subsidence can be detected using long-term SAR data and SAR interferometry techniques, and that this subsidence can be measured at the very least to an accuracy of a few centimeters.

Then we calculated the vertical displacement from the interferograms and compare it to the subsi-

dence of the correspond period from leveling results. Table 2 shows leveling data which are basically in agreement with interferogram. The correlation coefficient between InSAR observations and leveling observations is 0.943 and standard deviation is 0.1706, the accuracy of InSAR measurements is 5 mm. But there still exist some bias between InSAR value and leveling measurement. The principal sources of bias are (i) the loss of signal coherence in the change interferogram in areas where the radar backscatter characteristics have changed, (ii) the phase unwrapping error, and (iii) the position of benchmarks is not accurate.

Table 2. Comparison between interferogram and leveling data (1993～1995) over 41 benchmarks

Benchmark	InSAR value	Leveling value	Benchmark	InSAR value	Leveling value
IV1	0.006872	0.007	IV43	0.0012833	—
IV2	0.058380	0.032	IV46	0.0163142	—
IV3	0.037579	—	III1	0.0243299	0.023
IV5	0.032323	0.032	III2	0.0458992	0.040
IV7	0.005698	—	III3	0.0663299	0.066
IV9	0.128876	0.111	III4	0.0421639	—
IV11	0.021833	0.033	III5	0.0403959	—
IV13	0.125420	0.133	III6	0.0411693	0.042
IV16	0.040143	0.043	III7	0.0512087	0.038
IV17	0.033711	0.035	III8	0.0337761	0.032
IV21	0.055839	0.030	III9	0.0330612	0.034
IV23	0.038751	0.038	III10	0.0460612	—
IV25	0.031047	—	III12	0.0337669	—
IV28	0.029523	0.031	III13	0.0337731	0.034
IV31	0.036157	0.036	III16	0.0320103	0.030
IV32	0.007871	—	III17	0.0337681	0.034
IV33	0.007669	—	III18	0.0340702	—
IV36	0.104516	0.026	III19	0.0350043	0.038
IV37	0.042507	0.041	III20	0.0421474	0.034
IV38	0.034687	0.034	III21	0.0467762	0.034
IV42	0.038687	—			

—: no data.

Based on seven benchmarks, the subsidence rates were estimated (Fig. 1), the overall trend was in close agreement with D-InSAR results. The maximum subsidence rate is up to 8 cm/a, the average subsidence rate from 1993 to 1995 is 1.46 cm/a, the average subsidence velocity from 1998 to 2000 is less than 1 cm/a. The downtrend has been basically controlled through reducing groundwater exploitation to a large extent and by recharging of groundwater.

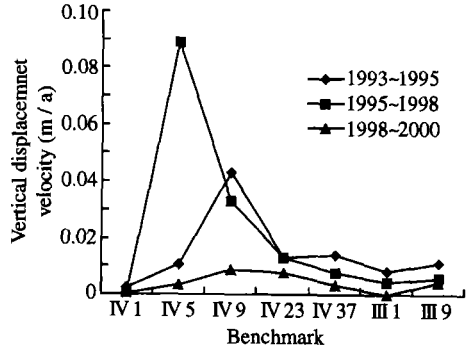

Fig. 1. Vertical displacement velocity obtained by SAR interferometry.

5 Conclusions

Land subsidence is a sinking of the land surface due to compression of the ground. In Suzhou it primarily results from groundwater overexploitation. Because of its spatially extensive nature it is a good candidate for measurement of SAR interferometry.

The qualitative comparison of the subsidence maps determined from ERS differential SAR interferometry and leveling surveys shows a very good performance of remote sensing techniques. The correlation between D-INSAR observations and leveling observations is 0.943 and standard deviation is 0.1706. Based on seven benchmarks, the subsidence rates have been estimated and the overall trend is in close agreement with InSAR results. We can conclude that for the mapping of land subsidence in urban environments InSAR has a strong potential for its cost-saving high resolution and accuracy. In many other cities affected by subsidence, InSAR should be operationally applied.

Acknowledgements The authors thank Academician Xu Guanhua, Professor Guo Huadong and Professor Huang Xiang for their support and advice. And other colleagues of this project are thanked.

References

1 Gabriel, A.K. et al. Mapping small elevation changes over large areas: differential radar interferometry. J. Geophys. Res., 1989, 94(B7): 9183.
2 Massonnet, D. et al. The displacement field of the Landers earthquake mapped by radar interferometry. Nature, 1992, 364: 138.
3 Zebker, H.A. et al. On the derivation of coseismic displacement fields using differential radar interferometry: The Lander earthquake. J. Geophys. Res., 1994, 99(B10): 19617.
4 Massonnet, D. et al. Land subsidence caused by the East Mesa geothermal field, California, observed using SAR interferometry. Geoph. Res. Lett., 1997, 24: 901.
5 Carnec, C. et al. Monitoring and modeling land sudsidence at the Cerro Prieto geothermal field, Baja California, Mexico, using SAR interferometry. Geoph. Res. Lett., 1999, 26: 1211.
6 Carnec, C. et al. Two examples of the use of SAR interferometry on displacement fields of small spatial extent. Geoph. Res. Lett., 1996, 23: 3579.
7 Wegmuller, U. et al. Validation of ERS differential SAR interferometry for land subsidence mapping: the Bologna case study. Proceedings of IGARSS'99, Hamburg, Germany, 1999.
8 Fielding, E. J. et al. Rapid subsidence over oil fields measured by SAR interferometry. Geoph. Res. Lett., 1998, 25(17): 3215.
9 Amelung, F. et al. Sensing the ups and downs of Las Vegas: InSAR reveals structural control of land subsidence and aquifer-system deformation. Geology, 27(6): 483.

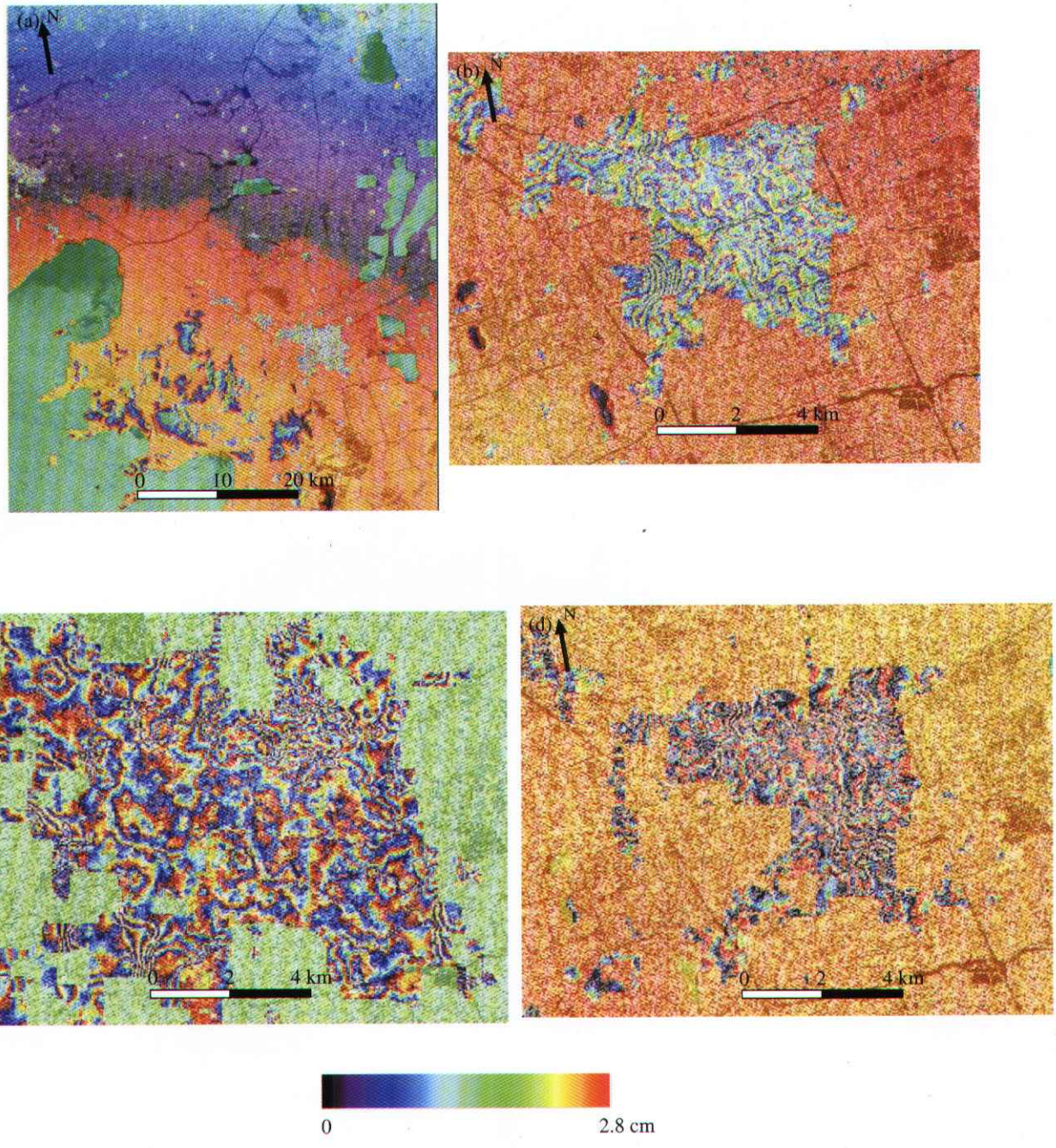

Plate Ⅰ. Differential interferograms for different time periods. (a) Subsidence from 1993 to 1995 in Suzhou area using ERS data, combined with ERS SAR backscatter data. A full color cycle corresponds to a displacement of the ground of 28 mm along radar look vector. (b) Subsidence map of urban area of Suzhou city (1993/02/25~1995/12/30). (c) Subsidence map of urban area of Suzhou city (1995/12/30~1998/04/19). (d) Subsidence map of urban area of Suzhou city(1998/04/19~2000/02/13).